NOISE-DRIVEN NEOCORTICAL INTERACTION: A SIMPLE GENERATION MECHANISM FOR COMPLEX NEURON SPIKING

R. Stoop[1], K. Schindler[1] and L.A. Bunimovich[2]

[1]Institut für Neuroinformatik, ETHZ/UNIZH, Winterthurerstr. 190, CH-8057 Zürich, Switzerland, phone/fax: 0041-16353063 or 52 (secretary), 0041-16353025
e-mail: ruedi@ini.phys.ethz.ch
[2]Southeast Applied Analysis Center, Georgia Institute of Technology, Atlanta GA 30332, USA

Received 4-II-1999

ABSTRACT

We discuss a generic scenario along which complex spiking behavior evolves in biologically realistic neural networks. Our nonlinear dynamics approach is based directly on rat neocortical *in vitro* recordings. Using this experimental data, we obtain a full overview on the possible spiking behaviors of pyramidal neurons that are engaged in binary interactions. Universality arguments imply that the observed spiking behaviors are largely independent from the specific properties of individual neurons; theoretical arguments and numerical experiments indicate that they should be observable in *in vivo* neocortical neuron networks.

1. INTRODUCTION

Neocortical circuits are formed of recurrently connected neurons. This is now a well-established fact, from both anatomical and physiological grounds (Douglas *et al.*, 1996). Cortical neurons are of two basic types, inhibitory and excitatory, and they are reciprocally coupled in monosynaptic or polysynaptic arcs. Their possible roles have been the subject of many analyses, both experimentally and theoretically (particularly in relation to visual receptive field properties). Relatively little attention has been given to the effect of such recurrent coupling on the global patterns of activity, although evidence from combined optical and single unit recordings of the primate visual cortex have indicated that single unit responses occur within quite complex global patterns of activity, and may vary from rather simple to complex behavior (Arieli *et al.*, 1996; Wilson and Cowan, 1972; An der Heiden, 1980). Consequently, the precise nature of this activity and its generating mechanisms remained mainly unexplained.

Related to this context, suggestions have been made that cortical networks may become chaotic under specific conditions (Schiff *et al.*, 1994; Mackey and An der Heiden, 1984; Pasemann, 1993, 1995a,b). However, at what level of description such a property can rigorously be established, where it originates from and what implications for the working brain this entails are difficult questions to answer. As a starting point, we were recently able to demonstrate that when recurrent excitatory-

Acta Biotheoretica **48**: 149–171, 2000.

inhibitory connections are activated experimentally, individual neurons exhibit both regular and chaotic firing patterns (Schindler *et al.*, 1997). In these *in vitro* experiments, regularly firing cortical neurons exhibit chaotic firing patterns when inhibitory pulses have a particular frequency relationship to the regularly firing neuron. The inhibitory input itself need not be chaotic at all; indeed it can be as regular as clockwork and nevertheless produce a chaotic firing pattern. However, statements on chaotic behavior obtained by numerical procedures often are of a treacherous nature. Questions like the length of transients or abundance of chaotic activity in the natural parameter space are generally difficult to answer at this level. To establish the claims on a firm ground, detailed analytical investigations are required.

In previous studies (Schindler *et al.*, 1997; Bernasconi *et al.*, 1999), we demonstrated that simple interneuron interactions can be described in a straightforward way by existing modeling tools (Hines, 1989, 1993). However, the correct modeling requires detailed knowledge of the values of many parameters, some of which are difficult to access. Furthermore, the real challenge is in extending such simple interactions to the scale of cortical networks. In this case, however, the computation times become exorbitant (Buzsáki and Chrobak, 1995; Wang and Rinzel, 1993). Therefore, to obtain more insight into the mechanisms that generate complex behavior in realistic neocortical networks, we chose an alternative strategy. Our approach follows methods of nonlinear dynamics established by Glass and Mackey (Glass *et al.*, 1984; Glass and Mackey, 1988) for cardiac cells. The advantage of this method is that it can be based directly upon experimental data, which drastically reduces the problem of choice of parameters. In the first part of the paper we give a description of our *in vitro* measurements of spiking neocortical rat neurons. These results are then used for the theoretical analysis of noise-driven biological networks. In the study, we concentrate on the following questions:

- What are the typical neuron firing patterns that emerge in biologically realistic neocortical networks, given the most simple stimulation paradigms? How stable and how abundant are these patterns; how much do they depend on the individual neuron characteristics?
- To what extent are these stimulation paradigms able to produce complex spiking behavior? What is the natural parameter-space measure of the expected chaotic response? Our analysis gives a complete answer to these questions:
- Realistic noise-driven networks self-organize towards complex behavior. This effect is established mostly through binary nearest-neighbor interaction.
- Inhibitory and excitatory binary interactions among rat neocortical pyramidal neurons are stable with respect to individual neuron variation. They are well described by circle-maps. Generated spiking patterns are organized along Arnold tongues which provide a complete overview of the spiking variability from both the topology and stability points of view. Numerical experiments and theoretical arguments indicate that the simple principles governing binary interaction remain valid under more complicated types of interaction.
- Chaotic activity is shown analytically to exist on a nonzero measure of the physiologically accessible parameter space and should, therefore, be experimentally observable.

The questions that we address are similar to the ones that were previously investigated by Hansel and Sompolinski (1996). These authors simulated hypercolumn models of the visual cortex to explain the differences between regular *in vitro* firing of

neurons (in response to a constant current injection) and irregular *in vivo* response. They concluded that the irregular firing is the result of synchronized chaos generated by the deterministic dynamics of local networks. In our alternative approach, we rely on directly measured data of neocortical neurons and we do not require a specific network architecture. We observe the same types of phenomena and are led to similar conclusions. However, our claims on the irregularity of the emerging spiking behavior are of a conceptually more fundamental and more mathematically precise nature.

2. NOISY NEURONAL INPUT

Consider neuronal input in a network with noise-dominated activity (e.g., in the absence of strong external stimulations from the sensory inputs). Due to the enormous number of synaptic contacts, a large number of small-strength synaptic inputs can be expected to arrive at the neuron (Abeles, 1982). Assuming a Gaussian central limit theorem behavior of the arriving input, the neuron receives an almost constant inflow of charge which can be represented by a constant driving current. Based on this assumption, our theoretical model allows us to establish a connection between realistic noise-driven *in vivo* neocortical networks, and *in vitro* rat neocortical neuron response. Our approach is similar to the mathematical idealization of the neuron made in the cable model (e.g., Hines, 1993), where the random walk aspects, generated by the random arrival of excitatory and inhibitory input, are neglected. Instead, the spiking behavior of the neuron is described by a limit cycle solution of the associated oscillator equations. Strong inhibitory or strong excitatory synaptic inputs correspond to a perturbation of this solution.

Rat neocortical pyramidal neurons indeed respond with a regular spiking behavior to a constant driving current (Abeles, 1982, Reyes and Fetz, 1993a,b). In the absence of other types of neuronal interaction, in noise-driven networks regularly spiking neurons would emerge, each one spiking at its own intrinsic frequency. However, self-organization sets in and modifies this picture: Neurons in close proximity are generally more strongly coupled than more distant ones, and the strength of interaction generally quickly decreases as a function of the topological neighborhood. Stronger synaptic input can also be generated by groups of synchronized neurons, or more generally, if substantial packages of spikes arrive at the neuron within a small time interval (Reyes and Fetz, 1993a,b). As a result, the formerly noise-driven neurons develop strong binary interactions that are no longer subject to the central limit theorem. Below, the binary interaction will be described as unidirectional. This point of view is consistent with the feed-forward characteristics of *in-vivo* biological neural networks. However, it does not prohibit bidirectional interaction; we merely assume that recurrent loops can be treated as secondary effects. The first question that we will address is: If a regularly spiking neuron is being perturbed by a neighboring neuron spiking at a different frequency, what is the form of the perturbed spiking pattern? Later in this paper, we will extrapolate our results to more complex types of interaction.

In our experiments with real neurons, slices of rat neocortex were prepared for *in vitro* recording. Following standard techniques, individual pyramidal neurons in layer 5 of barrel cortex were intracellularly recorded with sharp electrodes. To induce regular firing, a constant current was injected into the neurons (Reyes and Fetz, 1993a,b). The regular firing neuron was periodically perturbed by the extracellular stimulation of a synaptic input to the neuron. Excitatory perturbations were generated

by the stimulation of adjacent white or grey matter by means of bipolar electrodes. Inhibitory perturbations were generated when fast excitatory transmission was blocked pharmacologically, by application of 1:5 DNQX and AP5, and regular current pulses were applied to a fibre making a synaptic contact with the target neuron. In the context of *in vivo* neural networks, these perturbation paradigms can be regarded as the representation of synaptic inputs from strong synaptic connections (see, e.g., Reyes and Fetz, 1993a,b). For more details of the experimental set-up, preparation and recording see Schindler *et al.* (1997) and Schindler *et al.* (2000).

In Figure 1a we show a spike train $V(t)$ measured in this experiment. The first two spikes exhibit regular spiking behavior. The next two spikes show the response of the regularly spiking neuron, to strong perturbation represented by the strong downward deflection of the membrane potential V. In Figure 1b, the same spike train is shown as embedded data $\{V_i,\ V_{i-\tau}\}$, where $V_i \equiv V\ (t = t_i)$ and $V_{i+\tau} \equiv V\ (t = t_i + \tau)$ are the membrane potentials after an evolution of the system over time τ (τ is called the delay time, c.f. Peinke *et al.*, 1992). In Figure 1c we give a diagrammatic analysis of the embedded data. We isolate three regions of different dynamical behavior: a) channel motion with the fluctuations appearing in a random-like fashion (1,3,7); b) spike events (2); c) synaptic perturbations (4,5,6). In Figure 1d we show the channel motion at high magnification: In a random-walk manner the membrane potential is pushed towards the spiking threshold (this random-walk aspect is thoroughly discussed in a future contribution).

As is indicated by Figure 1a, the neurons show a nontrivial perturbation response. At a fixed perturbation strength, the spiking behavior depends in a nonlinear way on the *phase* $\phi := \frac{t_1}{T_0}$ at which the perturbation is applied (which indicates a strongly inhomogeneous random walk towards spiking threshold). This property is revealed by the *phase response function* $g(\phi)$. This function returns the ratio between the length of the perturbed interspike interval $T = T(\phi)$ and the length of the unperturbed interval T_0: $g(\phi) = \frac{T(\phi)}{T_0}$. In Figures 2a and 2b, dots show the measured perturbation response for inhibitory and for excitatory input, respectively. The phase response curves $g(\phi)$ (solid lines), are obtained by fits to this data set (we chose the simplest C^1-function for inhibition, while for excitation we found a piecewise linear approximation to be sufficient). Figure 2 shows two individual neuron responses, out from a collection of 200 cells that were experimentally investigated. In Figure 2a, missing data on the descending part of the curve at large phases might question the appropriateness of the fit. To obtain the behavior in this part, other cell responses have been taken into account. In other words, the two responses shown have been chosen as the characteristic results from the whole set of experimental data. In particular, it is a safe observation that the phase response curves are continuous, a result which is also corroborated by continued perturbation experiments (see below). Reyes and Fetz (1993a,b) described similar experiments. They measured a function that is closely related to our phase response function and obtained consistent results. In fact, our work can be seen as an extension of their approach. For the remainder of the paper, the two phase response curves shown in Figure 2 will be used in a paradigmatic way; deviations from these prototypical forms will be discussed in Section 3.

To obtain a more detailed description of the perturbed spiking behavior, we used the nonlinear dynamics approach originally proposed by Glass and Mackey (Glass *et al.*, 1984; Glass and Mackey, 1988).

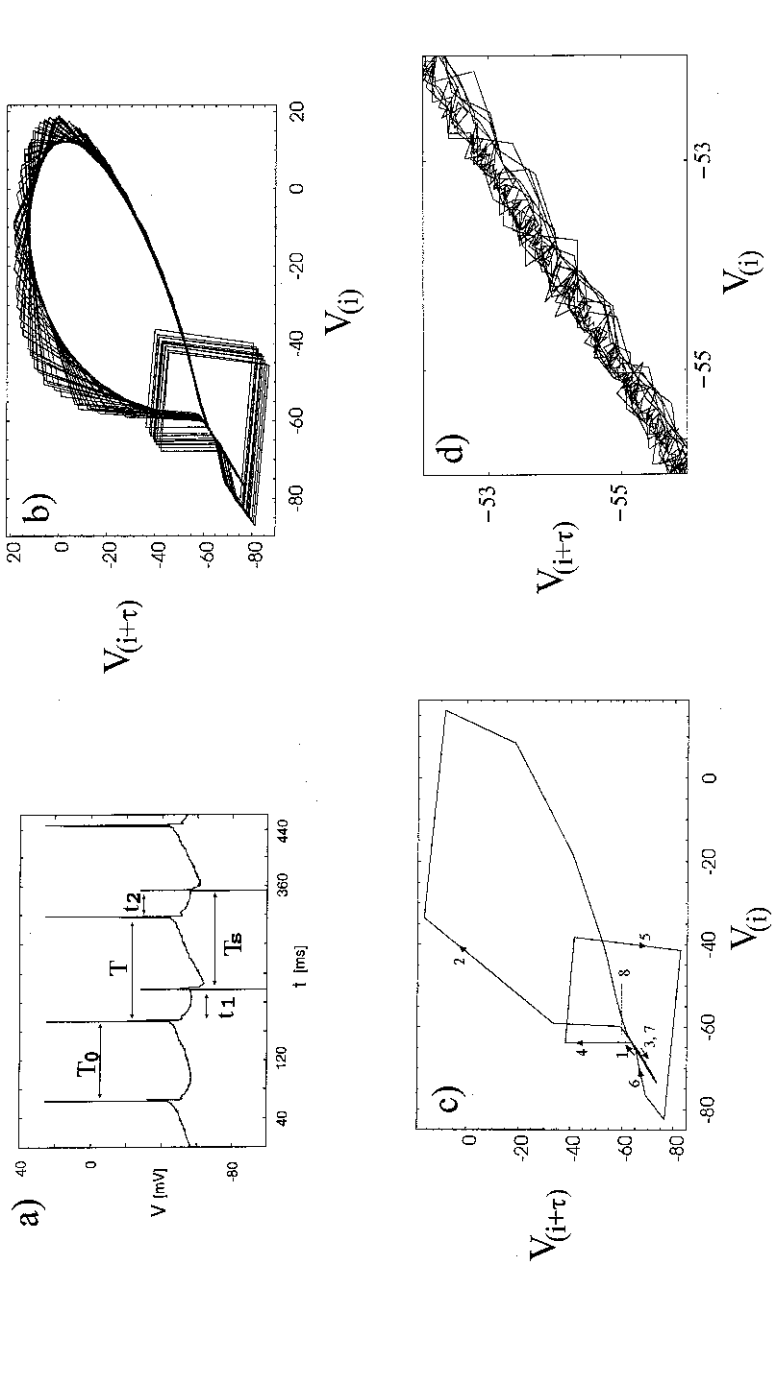

Figure 1. Different forms of results from a recorded *in vitro* rat neocortical neuron, without and with interaction with a neighboring neuron. a) experimental spike train, where inhibitory synaptic stimulation was applied. The symbols T_0, T, t_1, t_2, T_S allow the evaluation of the phase return map f_Ω. Due to inhibitory synaptic interaction with the neighboring neuron (characterized by two negative pulses), the former regular interspike time T_0 is now of variable length T. b) corresponding plot from embedded data $\{V_i,\ V_{i+\tau}\}$ (see text). c) diagrammatic analysis of Figure 1b: labels 1, 3 and 7: channel upward and downward motions, respectively; label 2: spike trace; labels 4-6: effect of synaptic perturbation; label 8: line of Poincaré section. In d) we zoom into the channel in order to uncover the random-walk aspects of the channel motion.

This approach is based directly on the measured phase response function $g(\phi)$. According to Figure 1a, for two successive perturbations we have:

$$T + t_2 = t_1 + T_S \tag{1}$$

where T_S is the perturbation period (i.e., the time between successive perturbations), $T = T(\phi)$ is the perturbed cycle length, t_1 is the time after spiking at which the perturbation was applied, and t_2 is the time after a spike event when the next perturbation arrives. To express this relation in terms of phases relative to the unperturbed cycle length T_0, we divide the equation by T_0. This leads to the equation

$$\phi_2 = \phi_1 + \Omega - g(\phi), \text{ mod } (1) \tag{2}$$

where $\Omega = T_S / T_0$ is the phase shift between the periodic limit cycle and the periodic perturbation and $g(\phi) = \frac{T(\phi)}{T_0}$, in accordance with the definition given above. Using for the unit interval the notation $I := [0,1]$, Equation 2 can be seen as defining a map on the circle (Cornfeld *et al.*, 1982)

$$f_\Omega(\phi_1) = \phi_2, \quad \text{where } \phi_1, \phi_2 \in I, \tag{3}$$

which will be called the *phase return map*. Geometrically, $f_\Omega: I \rightarrow I$ should be interpreted as a Poincaré return map (e.g., Peinke *et al.*, 1992). While in the usual Poincaré section approach, the location of the next intersection is of interest, here we focus on the time needed to reach the section, which is equivalent to the interspike interval length. It is worth emphasizing that in order to derive the phase response function, it is enough to consider single, isolated perturbations. Iteration (c.f. Section 6) of f_Ω, allows predictions to be made about the spiking behavior when the perturbation is repeatedly applied (=continued perturbations), provided that the stability of the limit cycles is strong enough (see Section 4).

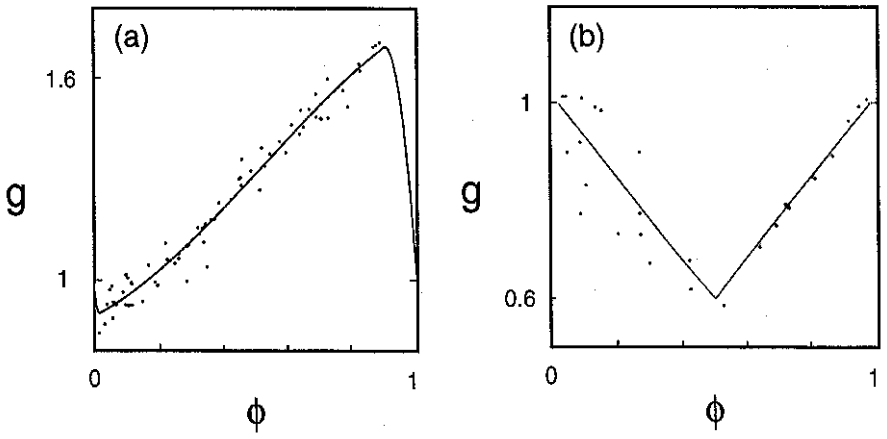

Figure 2. Response of a regularly spiking neuron to synaptic perturbation characterized by the *phase response function* $g(\phi)$ (Equation 2). The function measures how a perturbation delivered at phase ϕ modifies the length of the interspike interval. The dots represent the measured data from a neuron in the experiment of Figure 1: the solid lines show the associated interpolating functions. a) inhibitory; b) excitatory synaptic input. Note that inhibitory connections for early phases may yield an excitatory effect. Both experiments were performed at perturbation strengths that correspond to $K \sim 1$ (see Equation 4).

From numerical experiments with phase return maps it is immediately evident that the response of a regularly spiking neuron when subjected to regular perturbation, need not be regular. To make this observation more precise, we consider the set of phases $\{\phi_i\}$ that is generated by the iteration of map f_Ω. Regular spiking behavior is expressed by a finite cardinality p of this set. In this case, p is the periodicity of the spiking. However, p can also be infinite. Below we will investigate the dependence of p on the stimulus type (inhibition/excitation), on the stimulus strength K, and on the quality of the fit. We will also consider the influence of noise. In this way we obtain a complete overview on the spiking behavior of noise-driven neurons under binary interaction. Moreover, our description also provides a quantitative measure for the occurrence of the different spiking patterns.

3. COMPLEX BEHAVIOR OF THE NOISE-DRIVEN NETWORK: REGULARITY, STABILITY AND BIFURCATIONS

Displaying sets of iteratively generated phases as a function of Ω amounts to the generation of bifurcation diagrams (e.g., Argyris *et al.*, 1995). In Figure 3, phases $\{\phi_i(\Omega),\ i=1,..,n\}$ are plotted as dots in the vertical direction, for a set of equidistant values of the phase-shift Ω, where $n = 64$. At first view, the bifurcation diagrams seem to fall into two classes, depending on whether the phase response functions represent inhibitory or excitatory stimulation. Nevertheless, both bifurcation diagrams are typical for the circle-map universality class (Argyris *et al.*, 1995, and our Section 5). In Figure 4, the periodicities $p = card\{\phi_i(\Omega),\ i=1,..,n\}$ of the generated set of phases are shown as a function of Ω, at fixed stimulation strengths. As can be seen, in both cases the identical ordering of the periodicities emerges: In the horizontal direction, between an interval of period q (of winding number $\frac{p}{q}$) and a period $\hat{p}$ (of winding number $\frac{\hat{p}}{\hat{q}}$), always a period $q+\hat{q}$ (of winding number $\frac{p+\hat{p}}{q+\hat{q}}$) is found. In Figure 4a, the largest intervals correspond to periodicity 1 and the winding numbers $\frac{0}{1}$ and $\frac{1}{1}$, respectively. Between the two, an interval corresponding to periodicity 2 and winding number $\frac{1}{2}$ is found, and so on. This specific ordering of the periodicities is called the Farey-ordering (or Farey-tree). It ensures (provided the rule holds) the existence of all possible periodicities $p \in N$, where N denotes the set of positive integers. Identical Farey-tree structures emerge for the two types of stimulation. They indicate that the associated maps both belong to the circle-map class of one-dimensional maps (for more details see Section 5). In the next step we will point out how the dependence of the phase response function on the stimulation strength, which is denoted by K, can be included. We observed that, to reasonable accuracy, the perturbation of g is proportional to the physical stimulation strength K, for all phases ϕ. This dependence can be written as

$$g_{\Omega,K}(\phi) = g_{\Omega,Ko}(\phi - 1)\,K + 1, \tag{4}$$

where we chose the reference curve $g_{\Omega,Ko}$ at 75 percent of the maximally experimentally applicable perturbation strength (above the maximum threshold, continued perturbations cause irreparable damages to the cells). This functional dependence is based on a large number of perturbation response experiments using different stimulation strengths (for more detailed experimental results, see Schindler *et al.*, 2000). A plot of the emerging periodicities as a function of $\{\Omega,K\}$ is shown in

Figure 5, where colors code the values of p ($p \in \{1, ..., 9, \geq 10\}$ = {*orange*, *yellow*, *green*, ..., *red*}). For each fixed periodicity p, there are different (Arnold) tongues which comprise areas of the $\{\Omega,K\}$ parameter space having stable solutions of periodicity p. In fact, the Arnold tongues (e.g., Argyris *et al.*, 1995) are simply the extension of the Farey-tree structures of Figure 3 from the Ω- to the $\{\Omega,K\}$-space. For the different areas, the stability properties of the solutions are of interest. The Lyapunov exponent

$$\lambda_\Omega = \lim_{n\to\infty} \frac{1}{n} \log |(f_\Omega^{(n)})'(x_0)|, \tag{5}$$

where $f_\Omega^{(n)}$ denotes the n-fold iterate of f_Ω and x_0 is from the basin of attraction, are a measure of the stability of the orbits (Stoop and Meier, 1988). Positive Lyapunov exponents indicate chaotic behavior, negative exponents indicate stable behavior. Zero Lyapunov exponents are characteristic for marginal stability (Gaspard and Wang, 1988; Stoop, 1995a; Stoop, 1995b). Zooming into the picture shows that for the case of inhibitory stimulation, chaotic behavior is possible ($\lambda_{\Omega K} > 0$), but only for very strong input signals. Analytic investigations reveal that this occurs on an open set of nonzero Lebeque measure in the parameter space (see Section 6). In Figure 5, the parameterization by K (Eq. 4) has been used to extend the perturbation response beyond the biologically accessible parameter range (i.e., beyond the interval [0,1.33], see the normalization of K). Comparison of the bifurcation diagrams of inhibition and of excitation shows that the bifurcation structure for excitation is shifted towards high K-values. This implies that chaotic excitatory response could occur only at physiologically not accessible perturbation strengths. In fact, within the biologically meaningful parameter space, excitatory stimulations always yield invertible phase return functions. As non-invertibility is necessary for chaotic response, it follows that chaos cannot be generated from excitatory binary interaction. Integrate-and-fire models always yield invertible phase return maps, even when refractory periods are included. As a consequence, they are inappropriate for describing chaotic neuron response (Bernasconi *et al.*, 1999).

How strongly do our results depend on the fits made to obtain the phase response functions? The appropriate mathematical question requires a formulation in terms of universality properties of the circle-map class (this class is of a similar spirit to the better-known Feigenbaum class, c.f. Argyris *et al.*, 1995). It requires the evaluation of those variations of the phase response functions that are compatible with the circle-map class. *If* we remain within this class, then the universality principles of the class imply that all qualitative results remain unchanged, where "qualitative" comprises all topological properties of the results (e.g., structure of periods), as well as the property of producing positive or negative Lyapunov exponents, respectively (metric properties, e.g., widths of Arnold tongues, or exact size of Lyapunov exponents, may differ).

Our detailed analysis in Section 5 shows that the criteria for maps to belong to the circle-map class are of a surprising generality. The criteria even apply for the rather distinct phase response functions obtained for inhibition and for excitation (e.g., $g(\phi)$ is not differentiable in the excitatory case). Let us illustrate the strength of this property with examples. Suppose that in the case of excitatory stimulation, extended refractory periods are observed, and that this is strongly reflected in the associated phase response function $g(\phi)$ (in fact, this was the case for some of the investigated neurons). A simple numerical check provides immediate evidence that the

characteristic properties of our paradigmatic model are still valid. Or suppose that, for inhibitory stimulation, the experimental data is fitted by a) a polynomial of seventh order or b) by a piecewise linear map. Again, the results obtained are not only qualitatively similar to, but even hard to distinguish from Figures 3-5.

The strong universality features of the circle-map class also imply that higher resolution measurements of phase response functions do not contribute much to the understanding of the spiking patterns. It is true that a comparison between very accurate phase response functions from biophysical simulations and from experimental measurements can determine with a high precision some of the parameters involved in simulation models that are otherwise difficult to access (Schindler *et al.*, 1997). For a thorough understanding of the spiking behavior however, insight into the underlying mathematical principles is required. For that reason, in the more mathematical sections 5-6 we work out in detail the relevant theories. We will explicitly show how they can be applied to our experimental data, by taking into account the specific properties of the excitatory and of the inhibitory phase response functions, respectively.

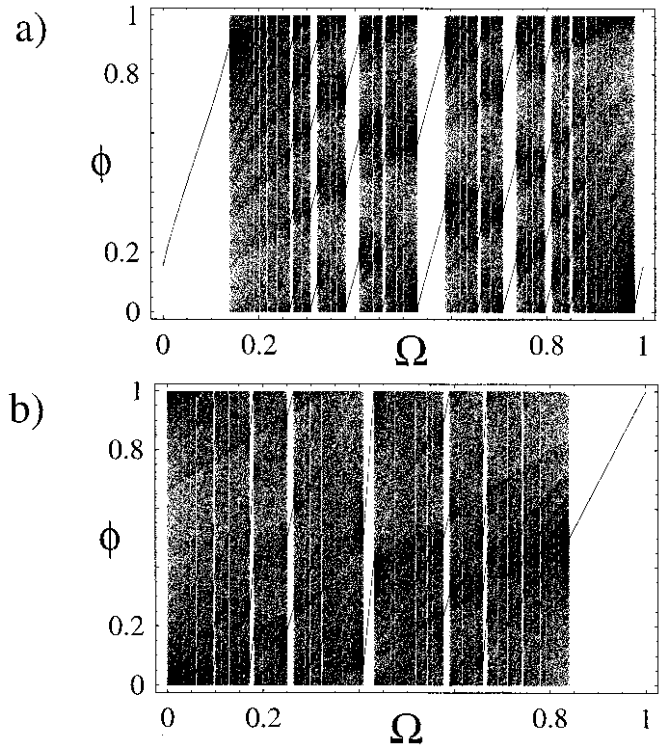

Figure 3. Bifurcation diagrams generated by f_Ω (Eq. 3), based on the phase response functions of Figure 2. Arbitrary initial conditions were iterated under f_Ω and the obtained phases were plotted using a fine grid for Ω (c.f. Eq. 2). For the stimulated neuron, the bifurcation diagrams seem to fall into two distinct classes, depending on whether the phase response function for inhibitory stimulation a), or for excitatory stimulation b), is considered (see text).

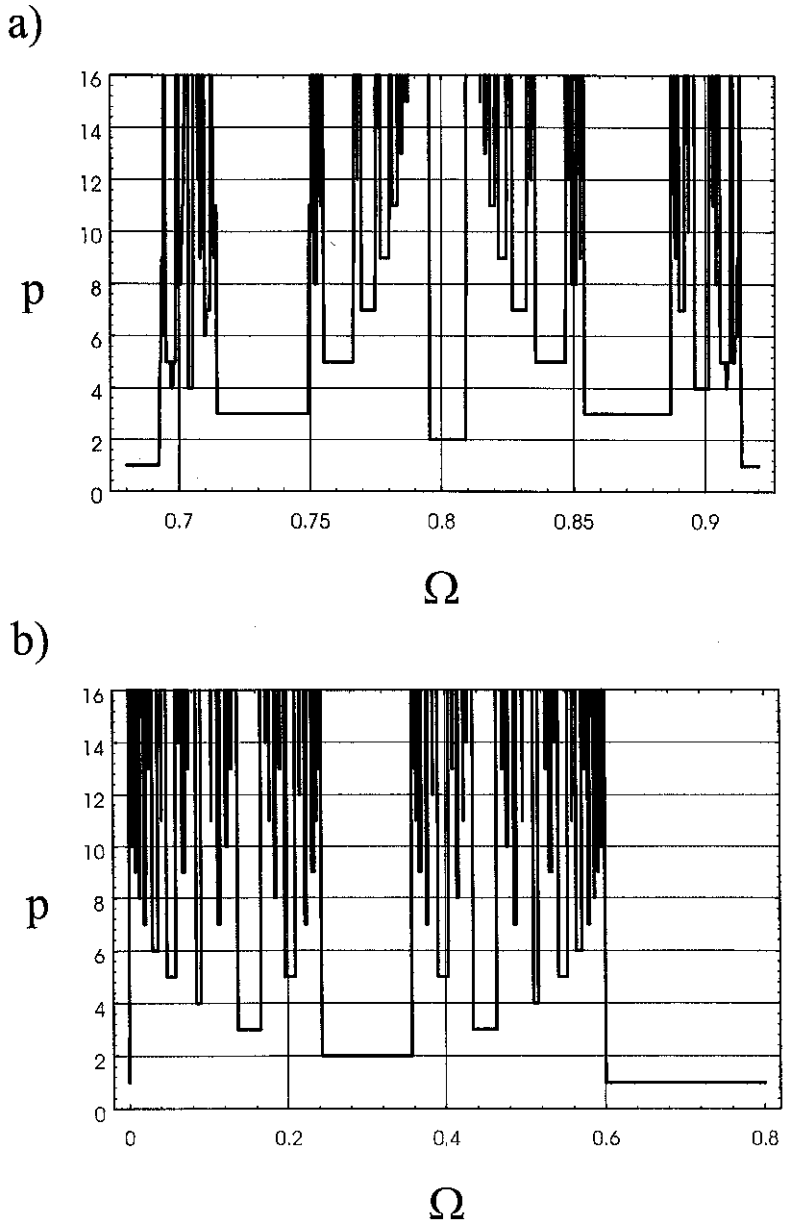

Figure 4. Periodic behavior of the perturbed neuron, at fixed stimulation strength K, for both types of stimulation. Shown is the periodicity p of the iterated dynamical map f_Ω, as a function of Ω. Any phase ϕ can be chosen as a starting point for the iteration. Both stimulations yield the same ordering of the periodicities, only metric properties (size of intervals) differ. a) inhibitory, b) excitatory case.

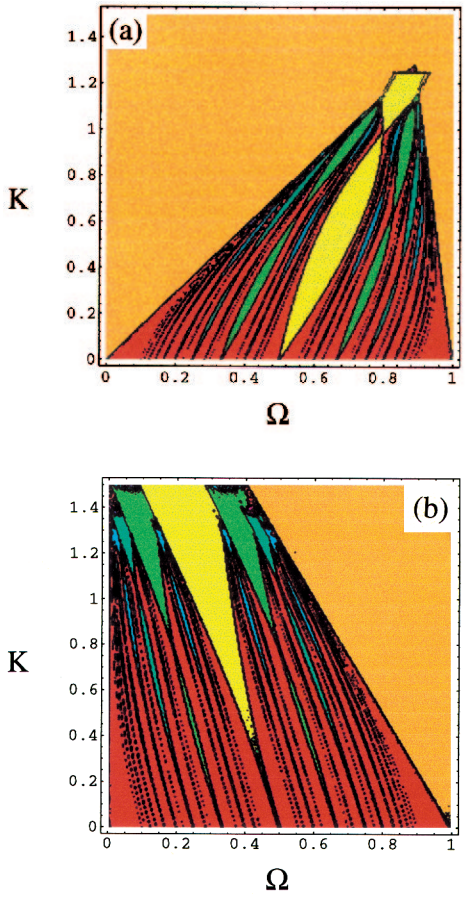

Figure 5. Experimental response of regularly synaptically perturbed regular spiking pyramidal cells. Results have been derived from Eq. 4 which allows extension beyond the biologically accessible range [0,1.35]. a), b) overview on the topological response of the neuron under perturbation, for variable perturbation strength K: So-called Arnold-tongue structures border the region of a given periodicity p in the $\{\Omega,K\}$-space (see text). Colors indicate the value of the periodicity $p \in \{1,\ldots,9, \geq 10\} = \{orange, yellow, green, \ldots, red\}$ of the asymptotic orbits. a) inhibitory, b) excitatory case. For optimal resolution, the calculation for inhibition was based on a piecewise linearization of the phase return map.

c), d) stability response of the neuron under perturbation: Lyapunov exponents calculated on the Arnold tongue structures measure the stability properties of the asymptotic orbits. The values of the exponent are plotted in the vertical direction. c) inhibitory, d) excitatory case. For inhibition, chaos is possible above $K \sim 0.95$; this value depends slightly on the form of the map. Chaos occurs first in small bands leading from smaller to larger K's, and is then prevalent in the top peak region of the triangle (calculations based on the function shown in Figure 2a). In the case of excitation, chaos cannot be reached by realistic values of K.

In experiments of continued perturbation, periods up to 5, sometimes 8, could consistently be resolved at the correct locations in the $\{K,\Omega\}$-space.

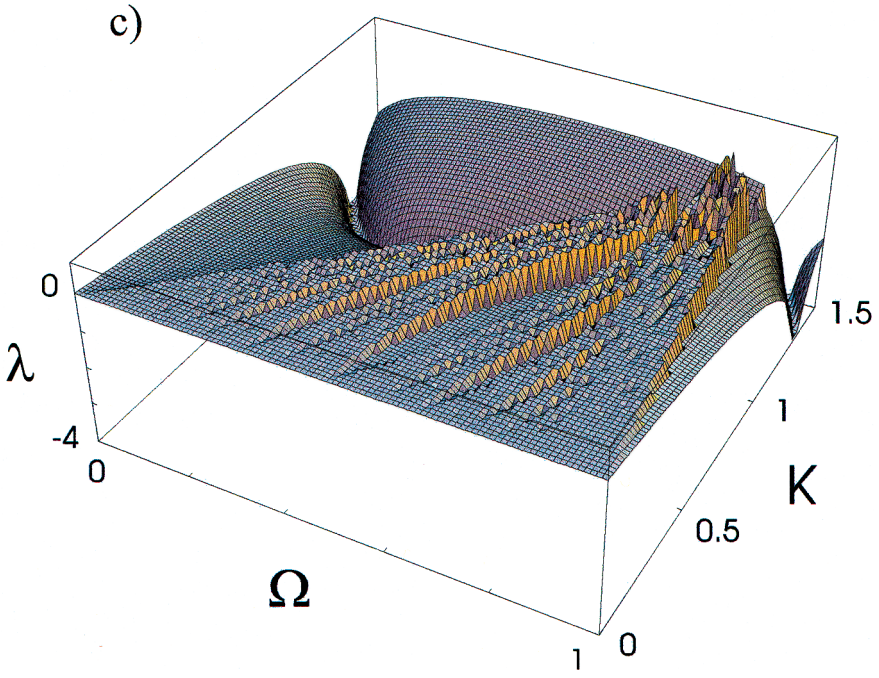
c)
0
λ
-4
0
Ω
1
0
0.5
1
K
1.5

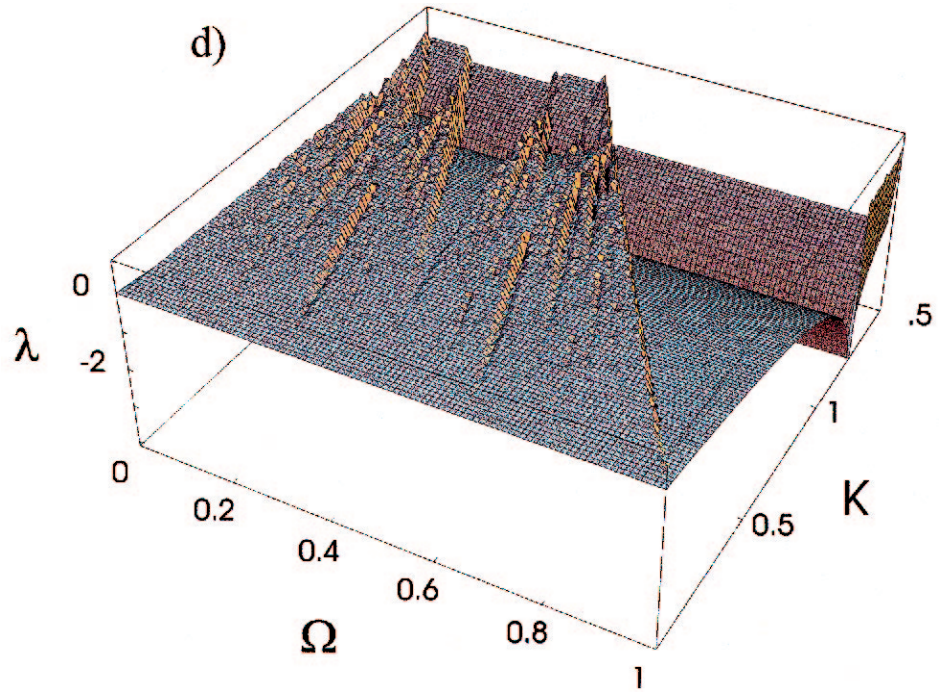
d)
0
λ
-2
0
0.2
0.4
0.6
0.8
Ω
1
0.5
1
K
.5

4. BEYOND NOISY DRIVING AND BINARY NEXT-NEIGHBORING INTERACTION

The ideal conditions for the observation of the predicted spiking behavior would be:

a) - no drastic changes in the excitabilities and in the intrinsic firing rates of neurons;

b) - sufficiently stable limit cycle behavior;

c) - fast exponential decay of interaction between neurons as a function of the neighboring order. This should restrict strong neural interaction essentially to (topological) nearest neighbors.

However, biologically realistic networks are not ideal. Let us consider how critical these conditions are to realistic networks. We start with condition b). For our statements on continued perturbations, the essential assumption is that the neuron is completely reset after firing. This property can be confirmed by comparing model predictions to experimental results of continued perturbations. In continued perturbations of the pyramidal neurons we identified periodic spiking behavior up to period 8 at the predicted values of Ω for intermediate stimulation strengths (see Schindler *et al.*, 2000). Higher periods that have a small basin of attraction are unresolvable due to the experimental noise. For a few cells, a very weak shortening of the interval following a perturbed interval was observed. However, this effect was small and did not accumulate. Our description of neuron firing by stable limit cycles also implies that the role of the noise should be small. Whereas our experimental pulse-perturbations showed traces of experimental noise, the nonlinear dynamics approach is able to describe the noiseless case. To estimate the strength of the experimental noise, we added Gaussian coloured noise to Eq. 2. We observed a smearing of the bifurcation structure that was monotonic with the strength of the added noise. Excellent agreement of the simulations with experimental results was obtained when the noise level was about 5% of the signal. We also observed that, as a general rule, single pulse perturbations indicate a significantly higher level of noise than what is actually observed in continued perturbation experiments, which we attribute to the very strong stability properties of especially the lowest Arnold tongues (c.f. Figure 5). In continued perturbations, we found *immediate* relaxation of the perturbed system to the asymptotic orbits (usually within one spike), which puts a very optimistic view on condition a). We, therefore, conclude that our assumption of a sufficiently stable limit cycle is well justified and that it is not unrealistic to expect stable neuronal activities on the relevant time-scales.

Condition c) seems to be the most critical one. Evidently, cortical interaction is not restricted to binary type. However, safe mathematical grounds exist to ensure qualitatively similar characteristics of neuron spiking patterns for ternary and higher interaction (Baesens *et al.*, 1991). Therefore, only evidence for the required separation of scales of synaptic input strength remains to be given. For realistic neural networks, we propose the following separation of synaptic inputs: 1. strong input, caused by the strongest connected next-neighbor neuron or by a group of synchronized neurons; 2. medium size input of longer periodicity or of chaotic nature, characterizing a structured environment and transmitted by means of, e.g., interneurons; 3. small-size, diffuse, decorrelated input, obeying the Gaussian law of large numbers. Expressed in

terms of the maximally applicable experimental stimulation strength (i.e., 4/3 K_0), we estimate these inputs to be of the order 10^{-1}, 10^{-2} and 10^{-4}, respectively, magnitudes, which would be consistent with our local approach. Although quantitatively only little is known about how well these scales separate in biologically realistic neural networks, there is widely accepted experimental evidence that synchronization and strong coupling play a major role in the organization of realistic neural networks (e.g., Abeles, 1982). To estimate the effects of medium-size perturbations on binary interactions, we generalized Eq. 4 to

$$f_{\Omega,K,\hat{K}} : \varphi_{n+1} = \varphi_n + \Omega - K(g(\varphi_n) - 1) + 1 - \hat{K}\sin(\omega_n) \tag{6}$$

where $\omega_{n+1} = \omega_n + \omega_0$ with fixed $\omega_0 = 0.1$ and $\hat{K} = 0.05$. In this way, the strength $\hat{K}$ of the secondary, deterministic, perturbation was of the order of 10% of the average of K. Orbit points were identified if they differed less than 10^{-2}. The results of this calculation are shown in Figure 6, where only the top region of the Arnold picture is displayed. They indicate that our approach should provide a good approximation to realistic neural networks.

As a first summary, the following behavior of realistic noise-driven cortical networks is suggested: Locally, low-periodic spiking behavior may be expected in abundance, by the interaction of otherwise freely spiking neurons. This periodic response is organized along Arnold tongues and obeys the circle-map class universality. Consequently, the network is able to respond locally with any desired periodicity (see Section 5). The presence of noise may restrict stable responses to the lowest, most stable, periods. While for weak local interaction the local spiking behavior is dominated by a wealth of different periodicities, for stronger interaction, there is a tendency for the response to settle towards more simple and more stable spiking patterns. These regular spiking patterns are in sharp contrast to the chaotic response which may emerge for strong inhibitory interaction. In Section 5 we will show that chaotic response exists on a nonzero Lebeque measure of the parameter space. This means that chaos should be observable and that systems could be tuned to such states. However, note that chaos requires comparatively strong stimulations and only occupies a small portion of the parameter space. Using the universality principles of the circle-map class, we are able to prove that our experimental observations do not depend on artificial preparation, but are "generic" for our set-up.

Also worth noting is that under ideal network conditions, information can only be efficiently encoded in terms of phases, not firing rates. This invites us to make a comparison between our results and earlier studies that concentrated on spike-timing reliability, i.e., on the potential of neuron interactions to generate reliable periodic spiking. This work has a long tradition. Most of the earlier works concentrated on Nitella, crayfish stretch receptors and mollusc neurons (for a collection of these early works see Degn *et al.* (1987)). Recently, this topic has once again become the subject of theoretical as well as of experimental interest. As a first step, Yarom (1991) was able to show that olivary neurons have the ability to generate sustained oscillations in neuron populations and that this ability seems to be restricted to a narrow frequency bandwidth. i.e., they are potential candidates for providing an accurate internal time reference for spike-time-critical cortical functions. Hayaishi and Ishizuka (1995) studied rat hippocampal slices in the CA3 region. In their experiments, they were able to clearly identify chaotic and phase-locked response under a mossy fiber stimulation, where their slices were heavily chemically prepared in order to serve as a model

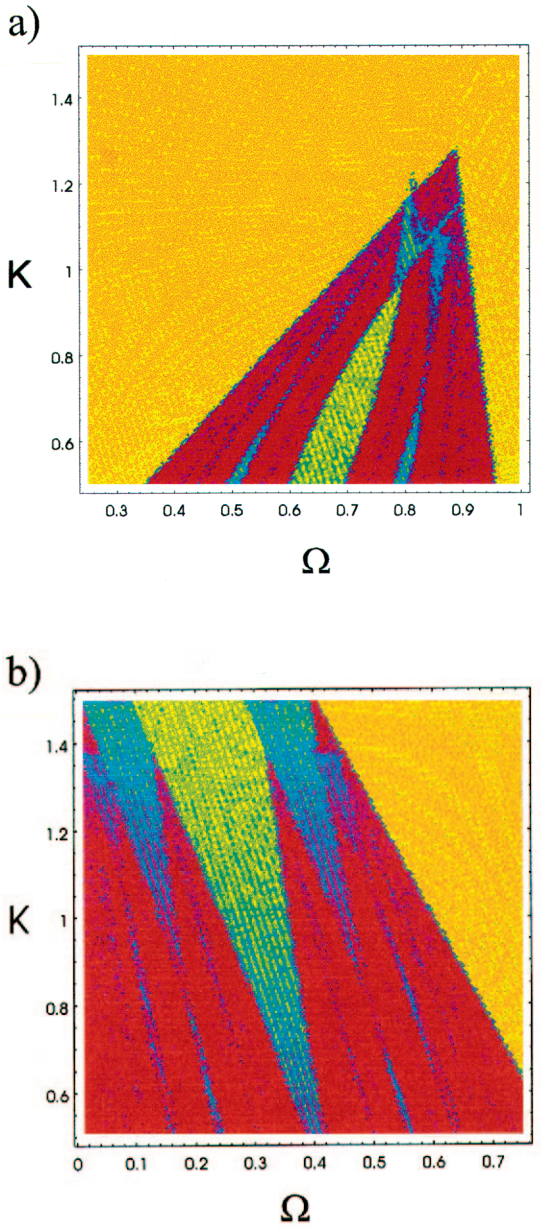

Figure 6. Form of the Arnold tongues of Figure 5, when an additional perturbation of more than 10 percent of the binary interaction is included. Note the close correspondence with the results of Figure 5. On this basis, we conclude that the described neuron response patterns should also be observed if the neuron pair is embedded into a network. a) inhibitory, b) excitatory case. Same coloring as in Figure 5.

for epileptogenesis. Hunter *et al.* (1998) investigated spike-timing reliability in Aplysia motoneurons, using integrate-and-fire neurons as theoretical models. Although these models are unable to express important response properties of pyramidal cells (Bernasconi *et al.*, 1999), their result that spike timing is reliable in the presence of noise only for frequency ratios that correspond to the lowest Arnold tongues, fully agrees with our numerical and theoretical findings. Actually, the requirement of a well-defined separation of the size of the synaptic input may be seen as an argument in favor of synaptic synchronization mechanisms. To make the concept work, the amount of noise should be smaller than the widths of the most relevant Arnold tongues. A similar point of view has recently been theoretically elaborated by Jensen (1998), who investigated the synchronization behavior of *randomly* forced oscillators. His finding was that (possibly nonperiodic) synchronization will be achieved, essentially if the differences of the frequencies do not exceed the width of the primary Arnold tongues, a result that places our approach on even more solid grounds.

In a forthcoming work, we also take into account the medium-size inputs. In our refined approach, a description by a lattice (Bunimovich and Sinai, 1988; Losson and Mackey, 1994) of binary interactions, on which medium-size input is represented by diffusive coupling, is appropriate. With this model, we are able to show that on the network level, the inhibitory connections contribute far more than excitatory connections to synchronization of the network. We have strong evidence that this conclusion remains valid far beyond our model. However, our insight into this interesting topic is entirely based on numerical simulations (there are mathematical reasons why analytical results cannot be expected).

5. TOPOLOGICAL RETURN-MAP PROPERTIES

The aim of this section and the next section is to provide the reader with a greater understanding of the nature and the mechanisms of the observed bifurcation structures, their topology and the stability properties of the associated orbits. While the results of the next section are entirely new, the aims of the discussion of the present section are twofold. Here, we present the mathematical theorems responsible for the topological structure of the neuron response and we also verify their applicability to our experiments. There is a conceptual difference between a map on the circle and a circle-map. The former term simply relates to the domain of a map, while the latter relates to a universality class of maps. In this section, we explicitly prove that our phase return maps are circle-maps. A very similar statement applies to the numerically observed chaotic response for inhibition. Although it is true that mode-locking leads naturally to a competition between different periodicities as the strength of interaction K increases (c.f. Glass and Mackey, 1988), the outcome of this competition depends on the properties of the map. To arrive at the statement of experimentally observable chaotic behavior, a separate discussion is required, which will be given in Section 6 (this situation is comparable with the Feigenbaum case). Beyond the limit of period doubling, chaos is *possible*, but may live on a set of measure zero. In this case, chaos would experimentally not be observable. The question of nonzero measure is not answered by the topological properties of the universality class alone; specific properties of the maps are needed for this discussion (see Stoop and Steeb, 1997).

To start the discussion of the topology of the phase return maps $f_\Omega(\phi)$ (Eq. 2), we first recall that $f_\Omega(\phi)$ depends on the nature of the stimulation of the cell (inhibitory

and excitatory stimulation, respectively). For both cases, *saddle-node bifurcations* (Argyris *et al.*, 1995) generate the bifurcation diagram. We now explain how the circle-map universality class generates the common structure behind the bifurcation diagrams. Our strategy of analysis is as follows. First, we concentrate on general features of the phase return maps, valid for both inhibitory and excitatory perturbation. The results are formulated in Theorem 1 which depends on Properties 1a and 1b. In these properties, metric aspects of the problem only play a marginal role. Therefore, the results apply for both stimulation paradigms. In the second part (appearing as Section 6), we focus on metric properties. In Theorem 2, we derive results on possible chaotic behavior of the phase return maps. The prerequisite for this theorem (Property 1c) however, is only satisfied in the case of strong experimental perturbations of the inhibitory type.

Property 1

a) The phase return map f_Ω is differentiable on I with exception of the point of discontinuity introduced by the modulo-operation in the definition of the phase and turning points in the linearized case. It has exactly two points x',x'' where its derivative $|f'_\Omega|$ equals one. Moreover, $|f'_\Omega| < 1$ on the segment $[x',x'']$ and $|f'_\Omega| > 1 \in I\backslash[x',x'']$. In the case of the linearized map, the corresponding points are the turning points.

b) f_Ω is onto I.

c) f_Ω is not injective on I.

Remark 1

Note that the Ω-dependence only results in a phase-shift. Properties 1a and 1b are satisfied by all maps that we consider (see Figure 2), in the differentiable nonlinear and also in the piecewise linear approximation case. Property 1c, which is not fulfilled by excitation for biological parameters, is needed for the generation of chaotic behavior. Condition 1b can be relaxed, if necessary.

Theorem 1

Let f_Ω satisfy the Properties 1a and 1b and violate Property 1c. Then the following holds true:

a) f_Ω generically has stable periodic orbits of all periods.

b) For every Ω, f_Ω has at most one stable periodic trajectory.

c) A stable periodic behavior of period p holds on an interval I_Ω^p of Ω-values.

Remark 2

A homeomorphism of a circle may have several stable periodic trajectories (in this case all of these trajectories must have the same period). However, this would require that the map has more than two points of derivative one, which is not the case, for both types of stimulations.

Proof

(Additional details to our arguments can be found in, e.g., De Melo and Van Strien, 1993.) For the excitatory case, the phase return map f_Ω is an orientation-preserving homeomorphism of the circle into itself, for all reasonable perturbation strengths. The rotation number is a monotonous function of Ω and for rational rotation numbers we have stable periodic orbits, that extend over a whole Ω-interval. As a consequence, we obtain the Farey-ordering (Argyris *et al.*, 1995), showing that all possible stable periodic orbits exist. For irrational rotation numbers, we have quasiperiodicity. Since the map is invertible in the experimentally accessible parameter space, the map is nonchaotic.

For inhibition, one may verify that the parameter K in Eq. 4 plays a role similar to the parameter K in the classical circle-map. For small K, the map is noncritical and the same statements hold as above. Increasing K leads the inhibitory case much faster to criticality. In this way, chaos can be achieved even for experimentally realistic values of K. The existence of a single stable solution on the interval is guaranteed as long as the maps are invertible.

Theorem 1 thus fully explains the topological structure of the observed bifurcation diagrams. Apart from producing an intricate bifurcation diagram, an important feature of the map accounting for inhibitory stimulation is its ability to produce chaotic motion, at appropriately chosen values of Ω. This feature will be analyzed in detail in the next section.

6. CHAOS VIA PEAK-CROSSING BIFURCATION

We now explain the mechanism that generates *experimentally observable chaotic behavior*. The generating mechanism is interpreted as a variant of the *peak-crossing bifurcation* (Bunimovich, 1995; Bunimovich and Ventakagiri, 1997). This strategy leads us to the statement that in the case of inhibition, the set of Ω-values producing chaotic behavior is of positive Lebeque measure. This means that the chaotic dynamics are experimentally observable and that the system can be prepared in order to produce such a behavior. The mechanism leading to chaos for inhibition is as follows (the strategy for maps of the excitatory type would be entirely different and simpler). Let $f_\Omega^{(n)}(x) := f_\Omega(f_\Omega(f_\Omega...(x)...))$ denote the n-fold iterated map of f_Ω. For inhibition, for all values of Ω, I has a natural partition into four segments I_1, I_2, I_3, I_4, whose end points are given by x', x'' in Property 1, and by the point $\hat{x}$ that yields a discontinuity of f as a map of the unit interval into itself (evidently, for excitation we have three segments I_1, I_2, I_3. Upon the identification of the initial and the final points of $I \to S^1$, I_1 and I_4 collapse into one segment, which shows that from the point of view of topology, a distinction between the inhibitory and the excitatory cases is unnecessary at this point). Denote by $\hat{x}$ the first nontrivial point of discontinuity on the interval. Depending on the value of Ω, point $\hat{x}$ may be situated inside the interval $[x', x'']$, so that generally we will have three points of discontinuity in the interval (there is always one exceptional value $\hat{\Omega}$ so that $f_{\hat{\Omega}}(I)$ is a continuous map from the unit circle into itself).

Given a large enough K, a chaotic motion occurs for some values of Ω in three bands of Ω. We denote by Ω_l^n, Ω_r^n the left and the right endpoints of the Ω-interval associated with a (stable) period n. For the sake of brevity we will only discuss in

detail the scenario in the band (Ω_r^3, Ω_l^1). The analogous bifurcation occurs in (Ω_r^1, Ω_l^2) and in (Ω_r^2, Ω_l^3), where the analysis is even simpler in the latter case. A typical graph of f_Ω for the case $(\Omega_r^1 \Omega_l^2)$ is shown in Figure 7.

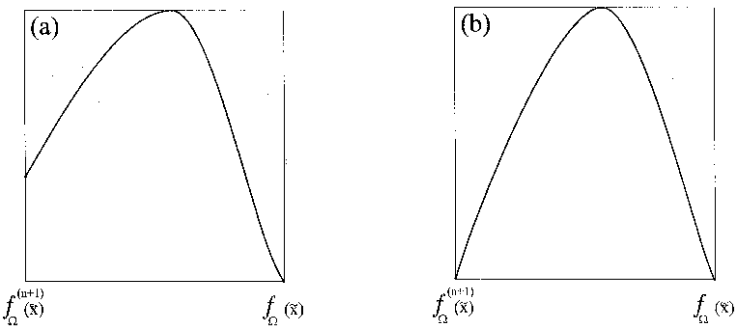

Figure 7 Relevant graph of f_Ω for inducing on the segment $[f_\Omega^{(n+1)}(\tilde{x}), f_\Omega^{(n)}(\tilde{x})]$. The on this interval induced map is the key tool for our analytical statement that in the case of inhibition, chaos dwells on set of nonzero Lebeque measure in the parameter space.

Denote by $\tilde{x}$ the unique critical point of f_Ω of the interval I_2. Let $f_\Omega^{(n)}(\tilde{x})$ be the first return of the (positively oriented) trajectory of $\tilde{x}$ to I_2. Suppose that $f_\Omega^{(n)}(\tilde{x}) > \tilde{x}$, which is possible for values $\Omega \in (\Omega_r^3, \Omega_l^1)$. Our next proposition is that $f_\Omega^{(2n)}(\tilde{x}) < \tilde{x} \in I_2$. Moreover, $f_\Omega^{(n+1)}(\tilde{x}) < f_\Omega^{(2n+1)}(\tilde{x}) < f_\Omega(\tilde{x})$ (see Figure 7). Consider now the interval $[f_\Omega^{(n+1)}(\tilde{x}), f_\Omega^n(\tilde{x})]$. The by $f_\Omega^{(n)}$ induced map on this interval has the graph as shown in Figure 8a. We denote the restriction of $f_\Omega^{(n)}$ to this interval by $\tilde{f}_\Omega^{(n)}$. Observe that for a fixed Ω the map $\tilde{f}_\Omega(x)$ is uniquely defined by $f_\Omega^{(n)}(x)$, provided that the above conditions are satisfied as in our case. The map $\tilde{f}_\Omega(x)$ belongs to the class of unimodal maps of an interval into itself. The properties of such types of maps are meanwhile completely understood (see Sinai, 1989; Lyubich, 1997). Given this situation, we arrive at the following statement:

Theorem 2

In each of the intervals (Ω_r^1, Ω_l^2), (Ω_r^2, Ω_l^3), (Ω_r^3, Ω_l^1) there exists a subset of a positive Lebeque measure on which the map $f_\Omega(x)$ has a positive Lyapunov exponent.

Proof

Suppose first Property 2: Let Ω be such that the condition $f_\Omega^{(2n+1)}(\tilde{x}) = f_\Omega^{(n+1)}(\tilde{x})$, is fulfilled, where $\tilde{x}$ is the above-defined critical point in I_2 (c.f. Figure 8b). In this case, for this Ω, the theorem is immediately clear. However, it is easy to see that there is only a countable set of values of Ω where this condition can be satisfied.

For the more general case (Figure 8a), fortunately a more sophisticated condition ensures that the positivity of the Lyapunov exponent holds for a set of positive measure of values of Ω (see for details Lyubich, 1997). This concludes our proof.

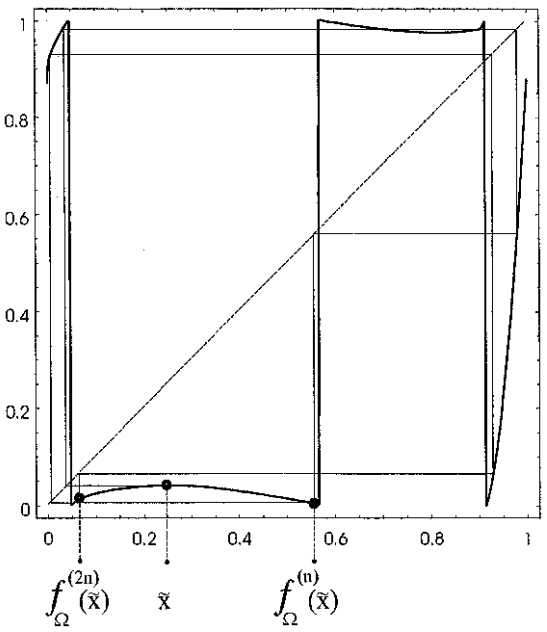

Figure 8. Generic and special graph of the by $f_\Omega^{(n)}$ on the segment $[f_\Omega^{(n+1)}(\tilde{x}), f_\Omega^{(n)}(\tilde{x})]$ induced map. For the special graph shown in Figure 8b, the argument for chaos of f_Ω on a set of nonzero Lebeque measure is straightforward. The generic case shown in Figure 8a requires a more careful analysis (see text).

7. CONCLUSIONS

We have determined the basic principles responsible for periodic and aperiodic spiking behavior in biological neural networks. We were able to formulate the topological and metric properties of the emerging spiking behavior in terms of mathematical existence and uniqueness theorems. In the regime where the neural network activity is dominated by small-scale noise and binary next-neighboring neuron interaction, this leads to a simple explanation of experimentally observed complex spiking behavior of neurons. Moreover, for this case we obtained a quantitative description of the natural abundance of the different periodic spiking patterns and we worked out the stability properties that they exhibit. Simulations and theory show that this quantitative description is valid for binary neuron interaction in a generic way.

From an information-theoretic point of view, the regularly perturbed neuron's potential to respond with stable periodic firing of any desired periodicity, is remarkable. The usual chaos control paradigm for the transmission of information (Ott *et al.*, 1990) starts from a chaotic ground state and then applies control techniques to arrive at a desired periodicity. The symbol to be transmitted is then encoded in terms of this periodicity, similar to the encoding by the ASCII table. In our case, both types of interaction can perform this task with ease, simply through a variation of the frequency or the stimulation strength of the sender, or by adjustment of the excitability of the receiver. In this interpretation, changes in the firing patterns which only affect

the value of Ω can be interpreted as rate-coding mechanisms, while changes mainly into the direction of K can be seen as synchronization effects.

Our investigations revealed how binary neuron interactions emerge locally within noisy networks of cortical neurons. We gave numerical evidence that the influence of medium-size input may be treated as a perturbation of dominant binary neuron interactions. Our final conclusion is that spiking patterns evoked by binary neural interaction should also be observable in *in vivo* activity, as subsystems embedded in the network activity. We recently successfully applied this approach to understand unexplained properties of *in vivo* interspike interval distributions (work unpublished). We expect similar spiking patterns to emerge from interactions between synchronized areas of the neocortex.

On the network level, we are confronted with our recent observation that there are significant differences between the influences on the network by inhibition and excitation, although the associated phase return maps belong to the same universality class of maps. In simulations of a refined model, in which phase coupling was included to represent medium-size inputs, we found that inhibition enhances synchronization much more than excitation. The reason for the efficacy of inhibition is beyond this contribution and will be addressed in the future. We also observed that when the strength of the phase-coupling is increased, the nature of the observed irregular behavior changes from local chaos to global turbulent behavior. This global turbulent behavior may correspond to the "synchronized chaos" observed by Hansel and Sompolinski (1996).

Finally, our insight into periodically perturbed regularly spiking cortical cells could be important for future hardware implementations of cortical cell response. For successful implementations, it may be necessary to understand how "real" data can be processed on top of the complex activity that we have shown to emerge. We need experiments on real and experimental noise-driven neural networks to understand how the real data features can be separated from the complex background activity.

ACKNOWLEDGEMENTS

This work was partially supported by the Swiss National Science Foundation and by KTI (contract Phonak). K.S. profited from support by the M.E. Müller foundation, Bern. We thank K.A.C. Martin for comments and critical reading of the manuscript. The authors acknowledge helpful discussions with Ya.G. Sinai. Special thanks go to N. Stoop for the preparation of the figures.

REFERENCES

Abeles, M. (1982). Local Cortical Circuits. Berlin: Springer.

Argyris, J., G. Faust and M. Haase (1995). Die Erforschung des Chaos. Braunschweig: Vieweg.

Arieli, A., A. Sterkin, A. Grinvald and A. Aertsen (1996). Dynamics of ongoing activity: Explanation of the large variability in evoked cortical responses. Science 273: 1868-1871.

Baesens, C., J. Guckenheimer, S. Kim and R.S. MacKey (1991). Three coupled oscillators: mode-locking, global bifurcations and toroidal chaos. Physica D 49: 387-475.

Bernasconi, C., K. Schindler, R. Stoop and R. Douglas (1999). Complex response to periodic inhibition in simple and detailed neuronal models. Neural Computation 11: 67-74.

Bunimovich, L.A. (1995). Coupled map lattices: one step forward and two steps back. Physica D 86: 248-255.

Bunimovich, L.A. and Ya.G. Sinai (1988). Space-time chaos in coupled map lattices. Nonlinearity 1: 491-516.

Bunimovich, L.A. and S. Ventakagiri (1997). On one mechanism of transition to chaos in lattice dynamical systems. In: R. Stoop and G. Radons, eds. Exact Approaches to Irregular Systems. Physics Reports 290: 81-100.

Buzsáki, G., and J.J. Chrobak (1995). Temporal structure in spatially organized neuronal ensembles: a role for interneuronal networks. Current Opinion in Neurobiology 5: 504-510.

Cornfeld, I.P., S.V. Fomin and Ya.G. Sinai (1982). Ergodic Theory. Berlin: Springer.

Degn, H., A.V. Holden and L.F. Olsen eds. (1987). Chaos in Biological Systems. New York: Plenum.

Douglas, R., M. Mahowald, K. Martin and K. Stratford (1996). The role of synapses in cortical computation. The Journal of Neurocytology 25: 893-911.

Gaspard, P. and X.-J. Wang (1988). Sporadicity: Between periodic and chaotic dynamical behaviors. Proceedings of the National Academy of Sciences USA 85: 4591-4595.

Glass, L., M. Guevara, J. Belair and A. Shrier (1984). Global bifurcations of a periodically forced biological oscillator. Physical Review A 29: 1348-1357.

Glass, L. and M. Mackey (1988). From Clocks to Chaos. Princeton: Princeton University Press.

Hansel, D. and H. Sompolinski (1996). Chaos and synchrony in a model of a hypercolumn in visual cortex. The Journal of Computational Neuroscience 3: 7-12.

Hayaishi, H. and S. Ishizuka (1995). Chaotic responses of the hippocampal CA3 region to a mossy fiber stimulation in vitro. Brain Research 686: 194-206.

an der Heiden, F. (1980). Analysis of Neural Networks. Berlin: Springer.

Hines, M. (1989). A program for simulation of nerve equations with branching geometries. International Journal of Biomedical Computation 24: 55-68.

Hines, M. (1993). The Neuron Simulation Program. In Skrzypek, J., ed., Neural Network Simulation Environments. Amsterdam: Kluwer.

Hunter, J.D., J.G. Milton, P.J. Thomas and J. Cowan (1998). Resonance effect for neural spike time reliability. Journal of Neurophysiology 80: 1427-1438.

Jensen, R.V. (1998). Synchronization in randomly driven nonlinear oscillators. Physical Review E 58: 6907-6910.

Losson, J. and M. Mackey (1994). Statistical cycling in coupled map lattices. Physical Review E 50: 843-856 (and further references given therein).

Lyubich, M. Yu (1997). Almost Every Real Quadratic Map is Either Regular or Stochastic. Preprint SUNYSB IMS.

Mackey, M.C. and U. an der Heiden (1984). The dynamics of recurrent inhibition. Journal of Mathematical Biology 19: 211-225.

de Melo, W. and S. van Strien (1993). One-dimensional dynamics. Berlin: Springer.

Ott, E., C. Grebogi and J.A. Yorke (1990). Controlling chaos. Physical Review Letters 64: 1196- 1199.

Pasemann, F. (1993). Discrete dynamics of two neuron networks. Open Systems and Information Dynamics 2: 49-66.

Pasemann, F. (1995a). Characterization of periodic attractors in neural ring networks. Neural Networks 8: 421-429;

Pasemann, F. (1995b). Controlling chaos. Physical Review Letters 64: 1196-1199.

Peinke, J., J. Parisi, O.E. Roessler and R. Stoop (1992). Encounter with Chaos. Berlin: Springer.

Reyes, A.D. and E.E. Fetz, (1993a). Two modes of interspike shortening by brief transient depolarizations in cat neocortical neurons. Journal of Neurophysiology 69: 1661-1672.

Reyes, A.D. and E.E. Fetz (1993b). Effects of transient depolarizing potentials on the firing rate of cat neocortical neurons. Journal of Neurophysiology 69: 1673-1683.

Schiff, St.J., K. Jerger, D.H. Duong, T. Chang, M.L. Spano and W.L. Ditto (1994). Controlling chaos in the brain. Nature 370: 615-620.

Schindler, K., C. Bernasconi, R. Stoop, P. Goodman and R. Douglas (1997). Chaotic spike patterns evoked by periodic inhibition in rat cortical neurons. Zeitung für Naturforschung 52a: 509-512.

Schindler, K., R. Stoop, C. Bernasconi, P. Goodman and R. Douglas (2000). Phase-locking induced by periodic inhibition of neocortical neurons, to appear (contains detailed experimental aspects, see also: Schindler, K.. Phil. Dr. Dissertation. University of Zurich. In preparation (1999)).

Sinai, Ya.G., ed. (1989). Dynamical Systems, Vol. 2, Enzyclopedia of Modern Mathematics. Berlin: Springer.

Stoop, R. (1995a). Thermodynamic approach to deterministic diffusion of mixed enhanced-dispersive type. Physical Review E 52: 2216-2219.

Stoop, R. (1995b). The diffusion-related entropy function: the enhanced case. Europhysics Letters 29: 433-438.

Stoop, R. and W.-H. Steeb (1997). Chaotic family with smooth Lyapunov dependence. Physical Review E 55: 7763-7766.

Stoop, R. and P.F. Meier (1988). Evaluation of Lyapunov exponents and scaling functions from time series. Journal of the Optical Society of America B 5: 1037-1045.

Stoop, R., K. Schindler and P. Goodman (1999). Chaotic firing of cortical neurons upon inhibitory periodic stimulation. In M.Barbi and S.Chillemi, eds. Chaos and Noise in Biological Systems, Ischia 1997. Singapore: World Scientific.

Wang, X.-J. and J. Rinzel (1993). Spindle rythmicity in the recticularis thalamic nucleus. Neuroscience 93: 899-904.

Wilson, H.R. and J.D. Cowan (1972). Excitatory and inhibitory interactions in localized populations of model neurons. Biophysical Journal 12: 1-24.

Yarom, Y. (1991). Rhythmogenesis in a hybrid system - Interconnecting an olivary neuron to an analog network of coupled oscillators. Neuroscience 44: 263-275.